2019 IEEE 4th International Conference on Signal and Image Processing

Underwater Image Enhancement by Gaussian Curvature Filter

Jiaying Xiong †, Yuxiang Dai†, Peixian Zhuang*
School of Electronic and Information Engineering
Nanjing University of Information Science and Technology,
Nanjing 210044, China
* Corresponding email: zhuangpeixian0624@163.com
† The co-first authors contributed equally.

***Abstract*—We develop a new Retinex-based variational model for enhancing single underwater image by imposing Gaussian curvature priors on the illumination and the reflection. Gaussian curvature filters are employed to estimate the illumination and the reflection efficiently for solving the proposed variational model. And Gaussian curvature filter can capture better underwater image details and prevent image over-enhancement. In addition, Gaussian curvature filter can reduce the runtime of underwater image enhancement without calculating both partial derivative operations and the gradient of overall energy functional. Ultimately, we provide numerous experiments to demonstrate the effectiveness of the proposed method, which outperforms several underwater enhancement algorithms in terms of enhancement performance, visual improvements and runtime.**

Keywords-Gaussian curvature filter; Retinex; Variational model formatting; Underwater image enhancement;

I. INTRODUCTION

Underwater image enhancement has aroused considerable attention both in computer vision and image processing. While light travels under water, low transparency and tiny particles lead to light energy attenuation at different levels, which suffers underwater images from color distortion, underexposure, and blurring [1]. And a large number of algorithms are developed to address these above problems. Galdran et al. [2] proposed an Automatic Red Channel method, which can be interpreted as a variant of dark channel method to avoid color artifacts resulting from wrong depth estimation. However, the enhanced image has details loss and border blurring. To promote image details, Ancuti et al. developed a wavelet-based fusion method [3] to overcome low contrast and color alteration, and Drews et al. presented a physical model of light propagation using statistical priors of the scene [4] which can recover medium transmission and scene depth for better visualization. Furthermore, Fu et al. presented a Retinex-based enhancing approach [5] for single underwater image, and an alternating direction optimization strategy is derived to solve the proposed variational model. Codruta et al. enhanced underwater images by fusing two images of color compensated and white-balanced [6], and the two images as well as their associated weight maps are fused to promote the transfer of edges and color contrast to the output image. Although the achievements of the aforementioned methods are obtained, these methods ignore geometric meaning of image details, and cannot capture better local gradient information. To address the above limitations, we develop a Retinex-based variational model for single underwater image enhancement with Gaussian curvature filter. The contributions of the proposed method can be summarized as below:

- A Retinex-based variational model, imposing Gaussian curvature priors on the illumination and the reflection, is proposed for single underwater image enhancement. And Gaussian curvature filters (GCF) are used to efficiently address the proposed model, which can capture better underwater image details and prevent image over-enhancement.
- Gaussian curvature filter has linear algorithmic complexity related to the number of image pixels without calculating the partial derivative and the gradient of the overall energy functional, which can reduce the runtime of underwater image enhancement.
- Numerous experimental results are provided by using two underwater metrics to demonstrate the effectiveness of the proposed model. Compared with several underwater enhancement methods, the proposed method yields better enhancement performance and visualization results.

II. METHOD

The proposed method includes four main steps: color correction [5], Retinex-based decomposition, Gaussian curvature filter (GCF) [8], and post-processing [5]. The proposed framework can be presented in Fig. 1 where we can see that the observed image appears color distortion, blurring and underexposure. It is noticeable that the visual improvements on the enhanced image using the proposed algorithm are obvious.

A. Color Correction

Most underwater images appear green or blue for light energy attenuation with different wavelengths [9]. To address color cast problems, we employ a simple but effective color correction method [5]. We calculate the mean and variance in RGB (red, green and blue) channels of the observed underwater image S respectively, and the maximum and minimum of each channel are obtained. Then the color corrected image is derived by.

$$H^{\sigma} = \frac{S^{\sigma} - S^{\sigma}_{min}}{S^{\sigma}_{max} - S^{\sigma}_{min}} \times 255$$
$$S^{\sigma}_{max} = S^{\sigma}_{mean} + \tau S^{\sigma}_{var} \quad (1)$$
$$S^{\sigma}_{min} = S^{\sigma}_{mean} - \tau S^{\sigma}_{var}$$

where $\sigma \in \{R, G, B\}$, S^{σ}_{var} and S^{σ}_{mean} are the variance and mean in the σ channel, τ is a free positive parameter to control the image dynamic. S^{σ}_{max} and S^{σ}_{min} are the maximum and the minimum of the channel respectively.

978-1-7281-3660-8/19/$31.00 ©2019 IEEE

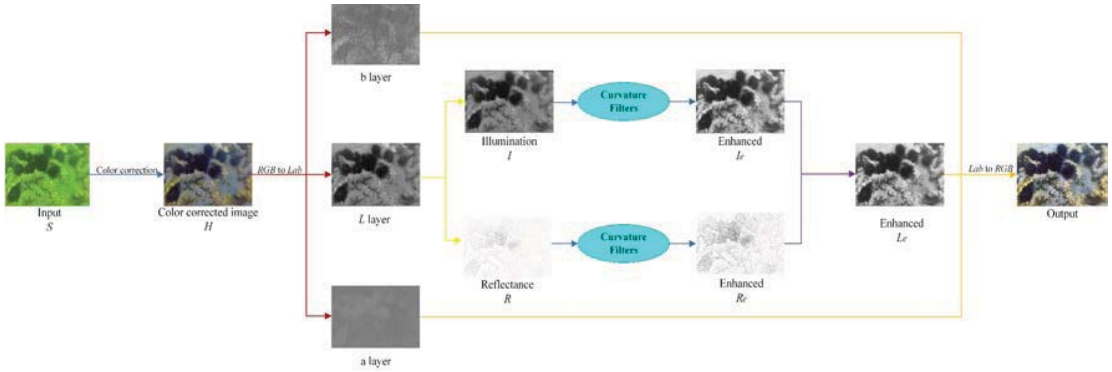

Figure 1: The flowchart of the proposed framework.

B. Retinex-based Decomposition

Since the variation of underwater environment is similar to the change of illumination, the Retinex method is employed to decompose the reflection(R) and the illumination(I) from the luminance layer L [10] - [13]. We propose a Retinex-based variational model by imposing Gaussian curvature priors on the R and I, which are estimated by GCF. Our model meets with the following conditions: ① R is piecewise constant since image edges and details exist, and I is piecewise smooth; ② L is a segmented surface; ③ The value of R is ranged in 0 and 1, which should subject to $I \geq L$. The proposed model can be finally established as:

$$\underset{R,\ I}{arg\,min} \int_{\Omega} (R \cdot I - L)^2 \, d\vec{\imath}\, d\vec{\jmath} + \rho \int_{\Omega} |K(R)| \, d\vec{\imath} + \mu \int_{\Omega} |K(I)| \, d\vec{\jmath} \quad s.t.\ L \leq I \tag{2}$$

where ρ and μ are positive parameters to balance R and I. $\vec{\imath} = (x, y) \in \Omega_R$, $\vec{\jmath} = (x, y) \in \Omega_I$ denote the space coordinates, and Ω_R and Ω_I represent a 2D image field of R and I. All calculations are component-wise operators. The data-fitting term $\|R \cdot I - L\|_2^2$ ensures the consistency between $R \cdot I$ and L. $\int_{\Omega} |K(R)| \, d\vec{\imath} = \int_{\Omega} K_1 K_2 \, d\vec{\imath}$, $\int_{\Omega} |K(I)| \, d\vec{\jmath} = \int_{\Omega} K_1 K_2 \, d\vec{\jmath}$, where K_1 and K_2 are the principal curvatures of the point on the surface. $K(R)$ and $K(I)$ are the alternative definitions of GC. Since the enhancement processing of R is same as that of I, we take the reflectance enhancement as an example, and its Gaussian curvature formula is:

$$K\big(R(\vec{\imath})\big) = \frac{R_{xx} R_{yy} - R_{xy}^2}{\big(1 + R_x^2 + R_y^2\big)^2} \tag{3}$$

where R_{xx}, R_{yy}, R_{xy}, R_x, and R_y are partial derivatives of R.

C. Gaussian curvature filter

For solving the models with Gaussian curvature (GC) priors, previous methods [20] [21] are limited in losing sharp edges and slow convergence. To overcome these issues, we utilize a filter that minimizes total absolute GC without ever explicitly computing GC. GCF [8] addresses this problem from the angle of differential geometry which makes full use of the discrete features of images and the continuous theory of differential geometry to obtain local known geometries. And the GCF solver reduces the regularization energy, and observes the data-fitting energy to stop alternative optimization in the situation that the data fitting energy always increases and the regularization energy always decreases. In addition, GCF can reduce the curvature energy without calculating the curvature and complex geometric flows for the reason that GCF is a local minimal projection operation, which could optimize their corresponding regularization terms and accelerate enhancement.

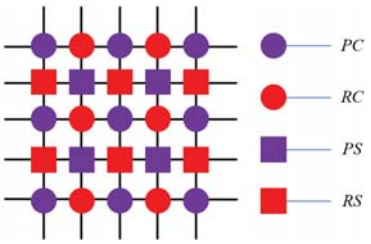

Figure 2: The sample space is decomposed into four sets.

We classify the discrete domain Ω_R of a reflectance R into two disjoint subsets: the red points and the purple points. We further split each of the two subsets: purple circle (*PC*), red circle (*RC*), purple square (*PS*), and red square (*RS*). All pixels in the same set are independent for the domain decomposition. The sample space (domain of definition) of the image can be seen in Fig. 2. Firstly, this decomposition ensures the independence between neighboring pixels. For example, when *PC* needs to be updated by the operator ϑ, all pixels in *PC* can be immediately updated. Secondly, the iteration order does not act on the pixels with independent sets, thus the update can use the updated neighbors with the guarantee of convergence. Thirdly, in a 3×3 local window, all possibilities can be enumerated in Algorithm 2, which means locally reducing the Gaussian curvature. Noting that $W(\vec{\imath}) = W(x, y)$ is the pixel value of (x, y) in the R, and $\widehat{W}(\vec{\imath})$ is the target intensity corrected by the operator of GCF ψ which is summarized in Algorithms 1 and 2. We denote this local update operation by ψ in Algorithm 2. Therefore, we perform the operator of ψ over all pixels in each of *PC*, *RC*, *PS* and *RS* by computing all $\{f_i, i = 1, \ldots, 8\}$ which can be used to make the surface $W(x)$ more developable. After computing all

$\{f_i, i = 1, \ldots, 8\}$, we find f_n such that $| f_n | = \min \{|f_i|, i = 1, \ldots, 8\}$. Then, we let $\widehat{W}(x,y) = W(x,y) + f_n$. This operator summarized in Algorithm 2 is compact and efficient because it only needs 36 operations (plus, minus, divide) for each pixel. After that, an alternating direction optimization algorithm is introduced to calculate R and I iteratively. The specific course is shown in Algorithm 3.

The specific calculation process is detailed as below:

Algorithm 1 GCF ϑ

Input: $W(x,y)$
1: $\forall \vec{x} \in BC, \psi(W(\vec{\imath}))$
2: $\forall \vec{x} \in BT, \psi(W(\vec{\imath}))$
3: $\forall \vec{x} \in WC, \psi(W(\vec{\imath}))$
4: $\forall \vec{x} \in WT, \psi(W(\vec{\imath}))$
Output: $\widehat{W}(x,y)$

Gaussian curvature algorithm is shown as follows:

Algorithm 2 Minimal Projection Operator ψ

Input: $W(x,y)$
1: $2\, f_1 = W(x-1,y) + W(x+1,y) - 2W(x,y)$
2: $2\, f_2 = W(x,y-1) + W(x,y+1) - 2W(x,y)$
3: $2\, f_3 = W(x-1,y-1) + W(x+1,y+1) - 2W(x,y)$
4: $2\, f_4 = W(x-1,y+1) + W(x+1,y-1) - 2W(x,y)$
5: $f_5 = W(x-1,y) + W(x,y-1) - W(x-1,y-1) - W(x,y)$
6: $f_6 = W(x-1,y) + W(x,y+1) - W(x-1,y+1) - W(x,y)$
7: $f_7 = W(x,y-1) + W(x+1,y) - W(x+1,y-1) - W(x,y)$
8: $f_8 = W(x+1,y) + W(x,y+1) - W(x+1,y+1) - W(x,y)$
Find f_n, such that $|f_n| = min\{|f_m|, m = 1, \ldots, 8\}$
Output $\widehat{W}(x,y) = W(x,y) + f_n$

Ultimately, the proposed algorithm is summarized:

Algorithm 3 Outline of Algorithm

Input: observed image S, parameters ρ and μ
Initialization: $I^0 \leftarrow$ Gaussian filtering of S
At the i-th iteration:
Update $R^i \leftarrow \vartheta(S/I^{i-1})$
Update $I^i \leftarrow \vartheta(S/R^i)$
Correct I^i using min (255, max (I^i, S));
Stop when the total energy no longer decreases
Output: enhancement R_e and I'

D. Post-processing

After alternative optimization of R and I, a post-processing method [5] is applied to solve the blurring problem. And contrast-limited adaptive histogram equalization (CLAHE) [14] is used to obtain enhanced reflectivity (R_e). Meanwhile, the histogram specification of the illumination (I') is improved to solve under-exposure problem. we constrain the area of the specified histogram in [15, 230], and calculate the enhanced illumination $I_e = Q(\Phi^{-1}(Q(I')))$. The cumulative density function (CDF) is revised:

$$Q\big(\Phi(\xi)\big) = \frac{\sum_{n=0}^{\xi} \kappa(n)}{\sum_{n=0}^{230} \kappa(n)} \tag{4}$$

where $\kappa(n) = \arctan(n-15), i \in [0,230]$. According to the definition of CDF [15] [16], the original formula is as follows:

$$Q(\theta) = \frac{\sum_{n=0}^{\theta} \tilde{I}\,(n) \cdot h(n)}{\sum_{n=0}^{\max(\theta)} \tilde{I}\,(n) \cdot h(n)} \tag{5}$$

where θ is the θ-th gray level of I, and h is the number of θ.

We can calculate the enhanced R and I, in which the enhanced layer L_e equals to $R_e \cdot I_e$. Finally, we convert Lab image to RGB image which is the final enhanced image.

III. EXPERIMENTAL RESULTS AND ANALYSIS

We provide numerous experiments to demonstrate the effectiveness of the proposed method. The proposed model is compared with five leading methods: RB [5], ARC [2], SUIE [17], mean curvature filter (MCF) and total variation filter (TVF), in which MCF and TVF are iterative-based methods. The codes of five competitive methods can be available on the authors' homepage. For assessing underwater enhanced results, we use two objective evaluation metrics: Underwater Color Image Quality Evaluation (UCIQE) [18] and Human-Visual-System-Inspired Underwater Image Quality Measures (UIQM) [19]. Higher values of UCIQE and UIQM demonstrate better enhancement results. And we investigate the sensitivity of the proposed algorithm about parameter settings by varying one parameter per-time when fixing the other at the current values. As shown in Fig. 5, the overall trend of weighting parameters μ and ρ first apparently increase and then tend to be steady. It is noted that the parameters ρ and μ are reasonably set to 6 and 180. Moreover, 3-5 iterations are empirically performed for satisfactory enhancement results.

To demonstrate the superiority of our method, we provide the visualization results of different underwater enhancement methods in Fig. 3. We can see that RB [5], ARC [2] and SUIE [17] present a certainly blurring across edges and uneven color backgrounds. Although these methods can reveal image details to some extent, their enhanced results are not pleasant enough (unclear textures, unnaturalness and color distortions). The proposed method yields a better visualization in recovering edges, textures and color correction, which are clearly not over-enhanced. In the third column of Fig. 3, our method achieves better color correction results, and in the fifth column of Fig. 3, our method achieves clearer edges and textures while other methods have slight over-enhancements which have been magnified in Fig. 4. As shown in Figs. 3 and 4, Gaussian curvature filter achieves better enhancement results than the other two curvature filters. Table 1 shows average mean and variance of UIQM and UCIQE for different enhancement methods on 50 underwater images, and our method obtains higher UIQM and UCIQE means than those of other methods, and the variances of GCF are comparable to those of MCF and TVF. In addition, TGV [7], MCF [8] and TVF [8] are considered to be the regularization term, and the three priors are respectively employed on the illumination and the reflection in our proposed variational framework. The runtime of our framework with the four priors are calculated on randomly selected 7 underwater images of different image sizes. As shown in Table 2, the proposed algorithm achieves a faster running time than other competitive methods.

IV. CONCLUSION

We have proposed a Retinex-based variational model where Gaussian curvature priors are imposed on the illumination and the reflection. Gaussian curvature filters are employed to efficiently address the proposed model, which can capture better image details and prevent over-enhancement. In addition, GCF has linear algorithmic complexity without calculating the gradient of overall energy functional and avoiding partial derivative operations. Moreover, numerous experiments demonstrate that the proposed method achieves better visual results, and our algorithm outperforms other competitive methods in subjective and objective assessments.

ACKNOWLEDGMENT

The authors would like to thank the anonymous reviewers for their helpful comments. This work was supported in part by the National Natural Science Foundation of China under Grant 61701245, in part by The Startup Foundation for Introducing Talent of NUIST 2243141701030, in part by A Project Funded by the Priority Academic Program Development of Jiangsu Higher Education Institutions, in part by College Students Practice Innovation Training Program of Nuist.

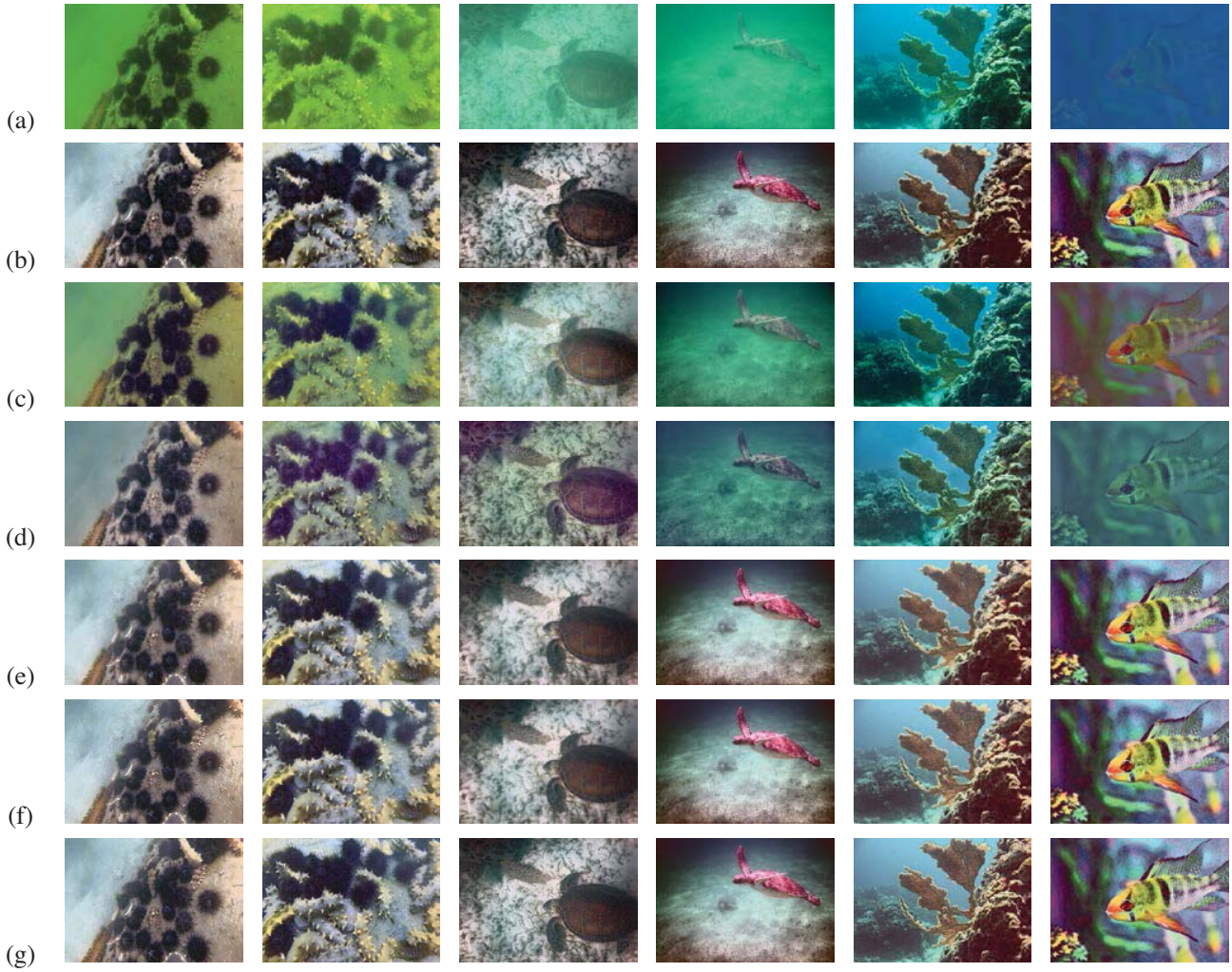

Figure 3: The enhancement results of different methods. (a) Raw images. (b) RB [5]. (c) ARC [2]. (d) SULE [17]. (e) MCF [8]. (f) TVF [8]. (g) Ours (GCF).

TABLE I: Average Mean/Variance of UIQM and UCIQE on 50 underwater images.

	Ours(GCF)	TVF [8]	MCF [8]	ACR [2]	RB [5]	SULE [17]
UIQM	**4.290301**/ 0.44745	3.967088/ **0.288441**	3.957755/ 0.502486	2.505141/ 2.63073	3.97022/ 0.585023	3.185825/ 1.889286
UCIQE	**0.58715**/ 0.001017	0.537229/ **0.000937**	0. 57986/ 0.000948	0.535985/ 0.00215	0.58405/ 0.001026	0.522049/ 0.004073

(a) (b) (c) (d) (e) (f) (g)

Figure 4: The partial enlargements of Fig. 3. (a) Raw images. (b) RB [5]. (c) ARC [2]. (d) SULE [17]. (e) MCF [8]. (f) TVF [8]. (g) Ours (GCF).

Table 3. The run time (s) of four variational methods on different image sizes.

Method	200×150	500×375	900×675	1000×750	1300×975	1600×1200	2000×1500
TVF	3.01	17.90	92.10	93.17	212.15	247.63	390.84
MCF	2.74	12.62	44.90	55.14	103.07	149.16	244.99
TGV	1.28	5.40	15.31	17.17	28.82	42.53	67.94
Ours(GCF)	**1.23**	**3.15**	**6.92**	**9.46**	**16.36**	**19.58**	**32.48**

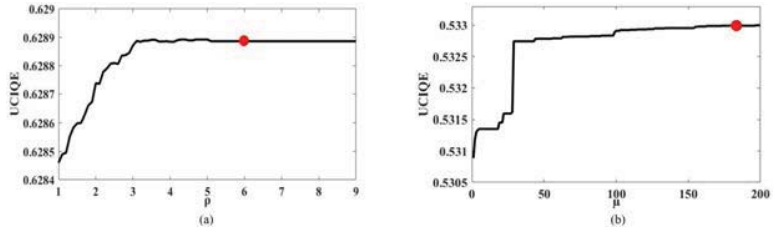

Figure 5: Parameter evaluation. (a) UCIQE versus ρ. (b) UCIQE versus μ.

REFERENCES

[1] M. Kocak., F. R. Dalgleish, F. M. Caimi, and Y. Y. Schechner, "A focus on recent developments and trends in underwater imaging." Marine Technology Society Journal 42.1, 2008, 52-67.

[2] A. Galdran , D. Pardo, and A. Picón, "Automatic red-channel underwater image restoration," Journal of Visual Communication and Image Representation, 2015, 26, 132-145.

[3] C. Ancuti, C. O. Ancuti, T. Haber, and P. Bekaert, "Enhancing underwater images and videos by fusion," IEEE Conference on Computer Vision and Pattern Recognition, 2012: 81-88.

[4] P. L. Drews, E. R. Nascimento, S. S. Botelho, M. F. M. and Campos, "Underwater depth estimation and image restoration based on single images," IEEE computer graphics and applications, 2016, 36(2), 24-35.

[5] X. Fu, P.Zhuang, Y. Huang, Y. Liao, X. P. Zhang, and X. Ding, "A retinex-based enhancing approach for single underwater image," IEEE International Conference on Image Processing (ICIP) October, 2014, pp. 4572-4576.

[6] C. O. Ancuti, C. Ancuti, C. De Vleeschouwer, P. and Bekaert, "Color balance and fusion for underwater image enhancement," IEEE Transactions on Image Processing, 27(1),2018, 379-393.

[7] K. Bredies, K. Kunisch, and T. Pock, "Total generalized variation," SIAM Journal on Imaging Sciences, 3(3), 2010, 492-526.

[8] Y. Gong and I. F. Sbalzarini, "Curvature filters efficiently reduce certain variational energies," IEEE Transactions on Image Processing, 26(4), 2017, 1786-1798.

[9] H. Lu, Y. Li, and S. Serikawa, "Underwater image enhancement using guided trigonometric bilateral filter and fast automatic color correction," IEEE International Conference on Image Processing, 2013, September, pp.3412-3416.

[10] E. H. Land, "The retinex. American Scientist," 52(2), 1964, 247-264.

[11] C. Tomasi, and R. Manduchi, "Bilateral filtering for gray and color images," In Iccv Vol. 98, No. 1, p. 2, January, 1998.

[12] E. H. Land, and J. J. McCann, "Lightness and retinex theory," Josa, 1971, 61(1), 1-11.

[13] G. Wyszecki, and W. S. Stiles, Color science Vol. 8, New York: Wiley, 1982.

[14] K. Zuiderveld, "Contrast limited adaptive histogram equalization," In Graphics gems IV August 1994,pp. 474-485.

[15] D. Coltuc, P. Bolon, and J. M. Chassery, "Exact histogram specification," IEEE Transactions on Image Processing, 2006, 15(5), 1143-1152.

[16] G. Thomas, D. Flores-Tapia, and S. Pistorius, "Histogram specification: a fast and flexible method to process digital images," IEEE Transactions on Instrumentation and Measurement, 2011, 60(5), 1565-1578.

[17] X. Fu, Z. Fan, M. Ling, Y. Huang, and X. Ding, November. "Two-step approach for single underwater image enhancement," IEEE International Symposium on Intelligent Signal Processing and Communication Systems (ISPACS),2017, pp.789-794.

[18] M. Yang, and A. Sowmya, "An underwater color image quality evaluation metric," IEEE Transactions on Image Processing, 2015, 24(12), 6062-6071.

[19] K. Panetta, C. Gao, and S. Agaian, "Human-visual-system-inspired underwater image quality measures," IEEE Journal of Oceanic Engineering, 2016, 41(3), 541-551.

[20] B. Lu, H. Wang, and Z. Lin, "High order Gaussian curvature flow for image smoothing," IEEE International Conference on Multimedia Technology, July,2011, pp. 5888-5891.

[21] D. Firsov, and S. H. Lui, "Domain decomposition methods in image denoising using Gaussian curvature," Journal of Computational and Applied Mathematics, 2006, 193(2), 460-473